

Supporting Information

© Wiley-VCH 2012

69451 Weinheim, Germany

**The Reaction of a High-Valent Nonheme Oxoiron(IV) Intermediate  
with Hydrogen Peroxide\*\***

*Joseph J. Braymer, Kevin P. O'Neill, Jan-Uwe Rohde,\* and Mi Hee Lim\**

ange\_201200901\_sm\_miscellaneous\_information.pdf

## Table of Contents

<b>Experimental Section</b>	S3
<b>Materials</b>	S3
<b>UV-Vis Spectroscopy</b>	S4
<b>ESI(+)<b>MS Measurements</b></b>	S4
<b><sup>1</sup>H NMR Spectroscopy</b>	S5
<b>EPR Spectroscopy</b>	S5
<b>O<sub>2</sub> Detection</b>	S6
<b>References</b>	S7
<b>Scheme S1.</b> Possible pathways to generate <b>6</b> in the reaction of <b>1</b> with an excess of H <sub>2</sub> O <sub>2</sub>	S8
<b>Figure S1.</b> UV-Vis spectra of the reaction of <b>1</b> with 0.5 equiv of H <sub>2</sub> O <sub>2</sub>	S9
<b>Figure S2.</b> ESI(+) mass spectra of <b>1</b> , <b>2</b> , and the products of the reaction of <b>1</b> with 0.5 equiv of H <sub>2</sub> O <sub>2</sub>	S10
<b>Figure S3.</b> <sup>1</sup> H NMR spectra of <b>1</b> , <b>2</b> , and the products of the reaction of <b>1</b> with 0.5 equiv of H <sub>2</sub> O <sub>2</sub>	S11
<b>Figure S4.</b> Control experiments for the detection of O <sub>2</sub> over time	S12
<b>Figure S5.</b> EPR spectra of frozen samples from the reaction of <b>1</b> with 0.5 equiv of H <sub>2</sub> O <sub>2</sub>	S13
<b>Figure S6.</b> Plot of <i>k</i> <sub>obs</sub> versus [ <b>1</b> ] for the reaction with H <sub>2</sub> O <sub>2</sub>	S14
<b>Figure S7.</b> Evidence for the formation of <b>6</b> in the reaction of <b>1</b> with excess H <sub>2</sub> O <sub>2</sub>	S15
<b>Figure S8.</b> Kinetic results for the reaction of <b>7</b> with H <sub>2</sub> O <sub>2</sub>	S16

## Experimental Section

**Materials.** All reagents were purchased from commercial suppliers and used as received unless stated otherwise. Acetonitrile (CH<sub>3</sub>CN), tetrahydrofuran (THF), dichloromethane (CH<sub>2</sub>Cl<sub>2</sub>), and diethyl ether (Et<sub>2</sub>O) were deoxygenated by sparging with N<sub>2</sub> and purified by passage through two packed columns of molecular sieves under an N<sub>2</sub> pressure (MBraun solvent purification system). Preparation and handling of air- and moisture-sensitive materials were carried out in a glovebox under an inert atmosphere of N<sub>2</sub>. Fe(OTf)<sub>2</sub>·2CH<sub>3</sub>CN (OTf = trifluoromethanesulfonate) was synthesized by a modified literature method from anhydrous FeCl<sub>2</sub> and trimethylsilyl trifluoromethanesulfonate in CH<sub>3</sub>CN and recrystallized from CH<sub>3</sub>CN/Et<sub>2</sub>O.<sup>[1,2]</sup> The compound [Fe<sup>II</sup>(N4Py)(CH<sub>3</sub>CN)](OTf)<sub>2</sub> [**2**(OTf)<sub>2</sub>, N4Py = *N,N*-bis(2-pyridylmethyl)-*N*-[bis(2-pyridyl)methyl]amine] was prepared following the previously reported procedure by addition of Fe(OTf)<sub>2</sub>·2CH<sub>3</sub>CN to a solution of N4Py in THF with a slightly modified work-up.<sup>[3,4]</sup> After stirring overnight, Et<sub>2</sub>O was used to precipitate the orange product, which was recrystallized from CH<sub>3</sub>CN/Et<sub>2</sub>O. The characterization of the Fe complex by <sup>1</sup>H NMR spectroscopy and electrospray ionization mass spectrometry (ESI MS) was in agreement with the previous report of **2**(ClO<sub>4</sub>)<sub>2</sub> (Figures S2 and S3).<sup>[3]</sup> The molar extinction coefficients for [Fe<sup>II</sup>(N4Py)(CH<sub>3</sub>CN)]<sup>2+</sup> (**2**) in CH<sub>3</sub>CN were 7.4 × 10<sup>3</sup> M<sup>-1</sup>cm<sup>-1</sup> (λ<sub>max</sub> = 380 nm) and 5.8 × 10<sup>3</sup> M<sup>-1</sup>cm<sup>-1</sup> (λ<sub>max</sub> = 454 nm) at 25 °C. [Fe<sup>II</sup>(tmc)(OTf)]OTf and iodosylbenzene (PhIO) were prepared by literature methods (tmc = 1,4,8,11-tetramethyl-1,4,8,11-tetraazacyclotetradecane).<sup>[5,6]</sup> Oxidation of the iron(II) complexes (stored in N<sub>2</sub> atmosphere) to the oxoiron(IV) complexes [Fe<sup>IV</sup>O(N4Py)]<sup>2+</sup> (**1**) and [Fe<sup>IV</sup>O(tmc)(CH<sub>3</sub>CN)]<sup>2+</sup> (**7**) was carried out with PhIO as reported.<sup>[5,7,8]</sup> Diluted aqueous solutions of hydrogen peroxide (H<sub>2</sub>O<sub>2</sub>) were used for standardizing its 50% (w/w) stock solution (Sigma Aldrich, St Louis, MO, USA) by UV-Vis spectroscopy (λ = 230

nm,  $\epsilon = 72.4 \text{ M}^{-1} \text{ cm}^{-1}$ ).<sup>[9]</sup> Deuterium peroxide ( $\text{D}_2\text{O}_2$ , 30% (w/w) in  $\text{D}_2\text{O}$ ) was purchased from Icon Isotopes (Summit, NJ, USA) and standardized using solutions diluted with  $\text{D}_2\text{O}$  in a similar manner to  $\text{H}_2\text{O}_2$ .

**UV-Vis Spectroscopy.** UV-Vis spectra were recorded on a Hewlett Packard 8453 diode array spectrophotometer with samples maintained at the desired temperature using a cryostat/heater from Unisoku Scientific Instruments (Japan). A typical reaction involved adding 50  $\mu\text{L}$  of a pre-chilled solution of  $\text{H}_2\text{O}_2$  (50% in  $\text{H}_2\text{O}$ ) in  $\text{CH}_3\text{CN}$  to a UV-Vis cuvette (path length, 1.0 cm) containing 2.0 mL of a solution of **1** or **7** in  $\text{CH}_3\text{CN}$  at  $-20$  or  $25$   $^\circ\text{C}$ , respectively. For experiments in a 0.1 cm UV-Vis cuvette, 10  $\mu\text{L}$  of a solution of  $\text{H}_2\text{O}_2$  in  $\text{CH}_3\text{CN}$  was added to 400  $\mu\text{L}$  of a solution of **1** in  $\text{CH}_3\text{CN}$ . Kinetic experiments for reactions of **1** with an excess of  $\text{H}_2\text{O}_2$  were monitored at 800 nm to reduce interference from other optical signals [*i.e.*, formation of  $[\text{Fe}^{\text{III}}(\text{N4Py})(\text{OOH})]^{2+}$  (**6**)]. Analysis of pseudo-first-order decay traces of **1** by plotting  $\ln A$  versus  $t$  indicated a linear trend for at least three half-lives. For the determination of the observed rate constant ( $k_{\text{obs}}$ ) under pseudo-first-order conditions, data were used from at least three (for **1**) or four (for **7**) experimentally determined half-lives. The fitting of kinetic data and determination of  $k_{\text{obs}}$  values for **1** and **7** were carried out using the ChemStation software (Agilent Technologies, Santa Clara, CA, USA). Values of  $k_2'$  were determined by dividing the second-order rate constant ( $k_2$ ) by the number ( $n$ ) of available protons for hydrogen atom transfer (for  $\text{H}_2\text{O}_2$ ,  $n = 2$ ). Kinetic experiments were carried out in triplicate.

**ESI(+)-MS Measurements.** ESI MS measurements were performed with a Micromass LCT time-of-flight mass spectrometer operating in the positive ion mode. Into a septum-sealed

4.0 mL vial, suspended in a cold bath at  $-20\text{ }^{\circ}\text{C}$  and containing a 1.0 mM solution of **1** in  $\text{CH}_3\text{CN}$ , was injected a solution of 0.5 equiv of  $\text{H}_2\text{O}_2$  in  $\text{CH}_3\text{CN}$ . Direct introduction of a sample from the reaction mixture into the mass spectrometer *via* a short transfer line was facilitated by applying slight pressure on the headspace of the solution with a syringe. Data were collected at a capillary voltage of 3100 V, a sample cone voltage of 17 V, a desolvation temperature of  $100\text{ }^{\circ}\text{C}$ , and a source temperature of  $100\text{ }^{\circ}\text{C}$ .

**$^1\text{H}$  NMR Spectroscopy.**  $^1\text{H}$  nuclear magnetic resonance (NMR) spectra were acquired with a Varian 400 MHz instrument at ambient temperature. The reaction of 1.0 mM **1** in  $\text{CD}_3\text{CN}$  with 0.5 equiv of  $\text{H}_2\text{O}_2$  at  $-20\text{ }^{\circ}\text{C}$  was monitored by UV-Vis spectroscopy. After no further spectral changes were observed at  $-20\text{ }^{\circ}\text{C}$  (*ca.* 4 h), the reaction solution was warmed to room temperature (no significant changes were observed in the optical spectrum upon warming). The orange solution was then analyzed by  $^1\text{H}$  NMR spectroscopy. The NMR spectrum of **1** in  $\text{CD}_3\text{CN}$  prior to the reaction with  $\text{H}_2\text{O}_2$  was consistent with that previously reported.<sup>[8]</sup>

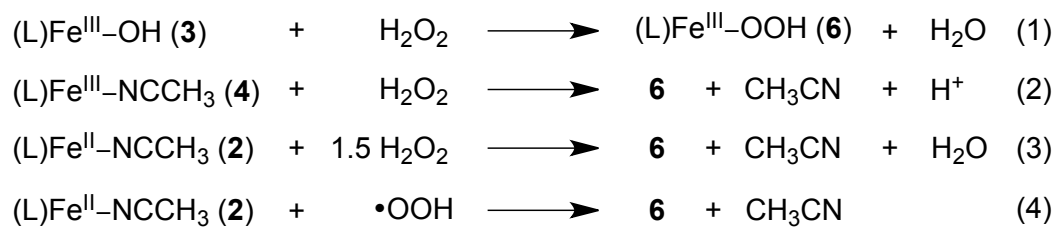
**EPR Spectroscopy.** Electron paramagnetic resonance (EPR) data were collected on a Bruker EMX electron spin resonance spectrometer equipped with an Oxford liquid helium cryostat or a Varian liquid nitrogen cryostat. For the preparation of EPR samples at different reaction time points, the reaction of 1.0 mM **1** in  $\text{CH}_3\text{CN}$  with 0.5 equiv of  $\text{H}_2\text{O}_2$  at  $-20\text{ }^{\circ}\text{C}$  was monitored by UV-Vis spectroscopy. At various time points, an aliquot of the reaction mixture was quickly transferred with a chilled Pasteur pipette into an EPR tube pre-cooled to  $-40\text{ }^{\circ}\text{C}$  and immediately frozen in liquid nitrogen. The EPR sample of  $[\text{Fe}^{\text{III}}(\text{N4Py})(\text{OH})]^{2+}$  (**3**) was prepared from the reaction of **2** (1.0 mM in acetone) with 0.5 equiv of  $\text{H}_2\text{O}_2$  at room temperature.<sup>[10]</sup> The

EPR spectra shown in Figure S5 were recorded at 4 K under non-saturating conditions with the instrument operating at 9.37 GHz, a power of 20.5 mW, a modulation frequency of 100 kHz, a modulation amplitude of 10 G, and a resolution in the X direction of 2048 points.

**O<sub>2</sub> Detection.** Concentrations of O<sub>2</sub> were measured using a borosilicate optical probe with 4.0 mm RedEye<sup>TM</sup> patches from Ocean Optics (Dunedin, FL, USA; HIOXY coating, calibrated for -20 to 25 °C and 0.0 to 8.0 ppm (mass/mass) of O<sub>2</sub>). The experiments were carried out in a threaded 1.0 cm cuvette (Starna Cells, Inc., Atascadero, CA, USA), containing 4.0 mL of solution to minimize headspace and sealed with a septum cap, at a temperature of -20 °C maintained by a cryostat from Unisoku Scientific Instruments. The borosilicate fiber optic probe was positioned with the RedEye oxygen sensing patch within the cuvette, and the entire set-up was then purged with N<sub>2</sub> to remove O<sub>2</sub>. The O<sub>2</sub> concentrations were measured upon injection of 100 μL of a thoroughly N<sub>2</sub> purged 0.02 M solution of H<sub>2</sub>O<sub>2</sub> in CH<sub>3</sub>CN *via* an air-tight syringe into either CH<sub>3</sub>CN only, 1.0 mM **1** in CH<sub>3</sub>CN, or 1.0 mM **2** in CH<sub>3</sub>CN. Concentrations were measured at various time points over 2 h at -20 °C. For experiments with 0.5 equiv of H<sub>2</sub>O<sub>2</sub> and 1.0 mM **1** or **2** in CH<sub>3</sub>CN, the reaction was continuously monitored by UV-Vis spectroscopy. As a control experiment, the concentration of O<sub>2</sub> in CH<sub>3</sub>CN in this set-up was measured over 2 h [0.9 (± 0.1) ppm], verifying minimal O<sub>2</sub> leakage into the cuvette. The measurements for O<sub>2</sub> detection were conducted in triplicate. A calibration curve was created at -20 °C using various concentrations (4.0 – 20 ppm) of O<sub>2</sub> with solutions prepared by dilution of an O<sub>2</sub> saturated CH<sub>3</sub>CN solution (8.1 mM O<sub>2</sub> in CH<sub>3</sub>CN at 25 °C).<sup>[11]</sup> The theoretical yield of 20.3 ppm of O<sub>2</sub> for the reaction of **1** with H<sub>2</sub>O<sub>2</sub> (based on a 2:1 stoichiometry between **1** and the produced O<sub>2</sub>) was found to correspond to a sensor reading of 13.7 (±0.4) ppm.

## References

- [1] J. Arnold, C. G. Hoffman, D. Y. Dawson, F. J. Hollander, *Organometallics* **1993**, *12*, 3645.
- [2] K. S. Hagen, *Inorg. Chem.* **2000**, *39*, 5867.
- [3] M. Lubben, A. Meetsma, E. C. Wilkinson, B. Feringa, L. Que, Jr., *Angew. Chem.* **1995**, *107*, 1610; *Angew. Chem. Int. Ed.* **1995**, *34*, 1512.
- [4] J.-U. Rohde, S. Torelli, X. Shan, M. H. Lim, E. J. Klinker, J. Kaizer, K. Chen, W. Nam, L. Que, Jr., *J. Am. Chem. Soc.* **2004**, *126*, 16750.
- [5] J.-U. Rohde, J.-H. In, M. H. Lim, W. W. Brennessel, M. R. Bukowski, A. Stubna, E. Münck, W. Nam, L. Que, Jr., *Science* **2003**, *299*, 1037.
- [6] H. Saltzman, J. G. Sharefkin, *Org. Synth.* **1963**, *43*, 60.
- [7] J. Kaizer, E. J. Klinker, N. Y. Oh, J.-U. Rohde, W. J. Song, A. Stubna, J. Kim, E. Münck, W. Nam, L. Que, Jr., *J. Am. Chem. Soc.* **2004**, *126*, 472.
- [8] E. J. Klinker, J. Kaizer, W. W. Brennessel, N. L. Woodrum, C. J. Cramer, L. Que, Jr., *Angew. Chem.* **2005**, *117*, 3756; *Angew. Chem. Int. Ed.* **2005**, *44*, 3690.
- [9] P. George, *Biochem. J.* **1953**, *54*, 267.
- [10] G. Roelfes, M. Lubben, K. Chen, R. Y. N. Ho, A. Meetsma, S. Genseberger, R. M. Hermant, R. Hage, S. K. Mandal, V. G. Young, Jr., Y. Zang, H. Kooijman, A. L. Spek, L. Que, Jr., B. L. Feringa, *Inorg. Chem.* **1999**, *38*, 1929.
- [11] S. V. Kryatov, E. V. Rybak-Akimova, S. Schindler, *Chem. Rev.* **2005**, *105*, 2175.



**Scheme S1.** Possible pathways to generate **6** when an excess of  $\text{H}_2\text{O}_2$  is present in the reaction with **1** (Scheme 1).



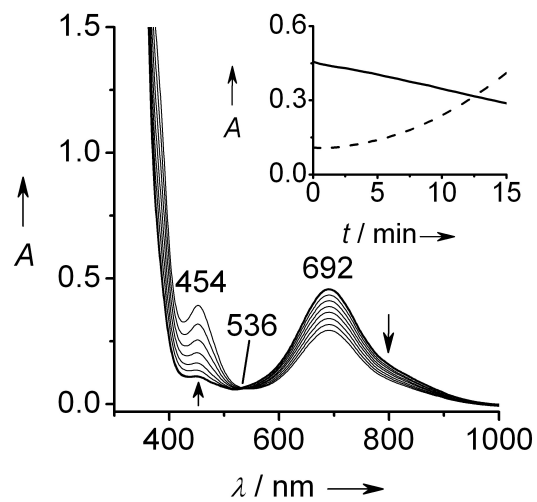
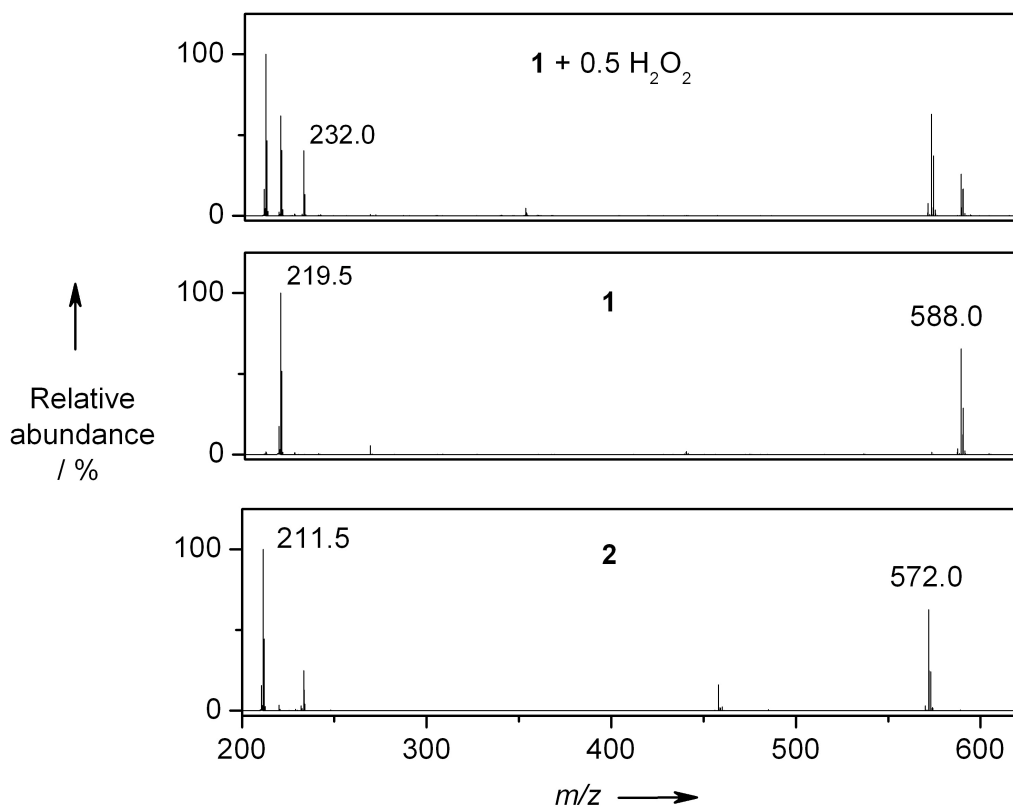


**Figure S1.** UV-Vis spectra of the first 15 min of the reaction of 1.0 mM **1** in CH<sub>3</sub>CN (bold line) with 0.5 equiv of H<sub>2</sub>O<sub>2</sub> at -20 °C (path length, 1.0 cm; cf. Figure 1). Inset: Time courses of the decay of **1** ( $\lambda = 692$  nm, solid line) and the formation of **2** ( $\lambda = 454$  nm, dashed line).



Species	Observed ( <i>m/z</i> )	Calculated ( <i>m/z</i> )
$[\text{Fe}^{\text{II}}(\text{N4Py})]^{2+}$	211.5	211.6
$\{[\text{Fe}^{\text{II}}(\text{N4Py})] + \text{CH}_3\text{CN}\}^{2+}$	232.0	232.1
$\{[\text{Fe}^{\text{II}}(\text{N4Py})] + \text{OTf}\}^+$	572.0	572.1
$[\text{Fe}^{\text{IV}}\text{O}(\text{N4Py})]^{2+}$	219.5	219.5
$\{[\text{Fe}^{\text{IV}}\text{O}(\text{N4Py})] + \text{OTf}\}^+$	588.0	588.1

**Figure S2.** ESI(+) mass spectra of **1**, **2**, and the products of the reaction of 1.0 mM **1** in CH<sub>3</sub>CN with 0.5 equiv of H<sub>2</sub>O<sub>2</sub> at -20 °C (top) and summary of the observed and calculated *m/z* values (bottom).

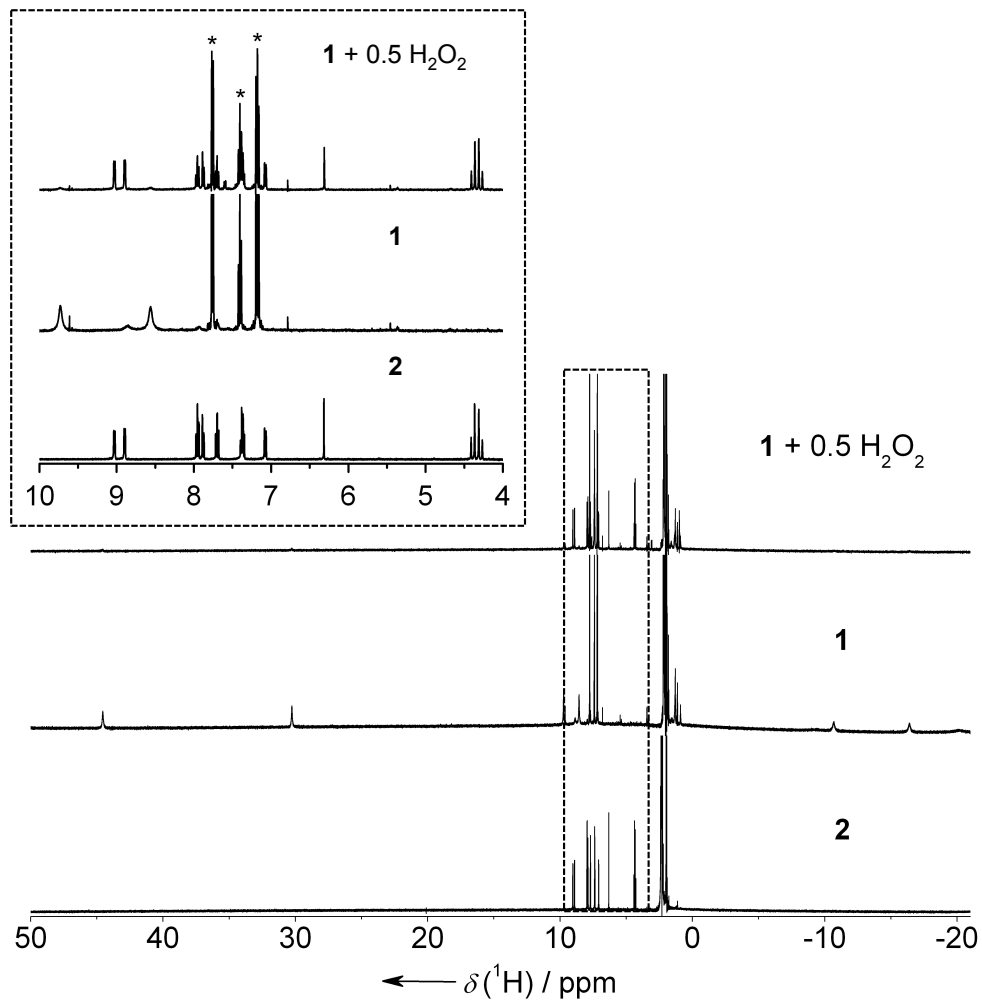


**Figure S3.**  $^1\text{H}$  NMR spectra of **1**, **2**, and the products of the reaction of 1.0 mM **1** with 0.5 equiv of  $\text{H}_2\text{O}_2$  ( $-20\text{ }^\circ\text{C}$ ) in  $\text{CD}_3\text{CN}$ . Spectra were recorded at room temperature (400 MHz). Inset: Expanded view of the region from 4 to 10 ppm. The asterisks (\*) indicate the  $^1\text{H}$  NMR signals of iodobenzene.

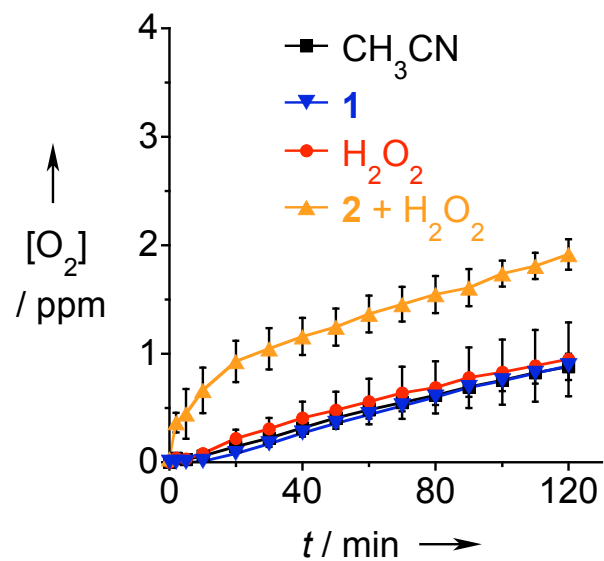


**Figure S4.** Control experiments for the detection of O<sub>2</sub> over time in CH<sub>3</sub>CN (black squares), in a 1.0 mM solution of **1** in CH<sub>3</sub>CN (blue inverted triangles), and upon addition of 100 μL of a 0.02 M solution of H<sub>2</sub>O<sub>2</sub> (in CH<sub>3</sub>CN) to CH<sub>3</sub>CN (red circles) and to 1.0 mM **2** in CH<sub>3</sub>CN (orange triangles). The measurements were conducted at −20 °C and in triplicate.

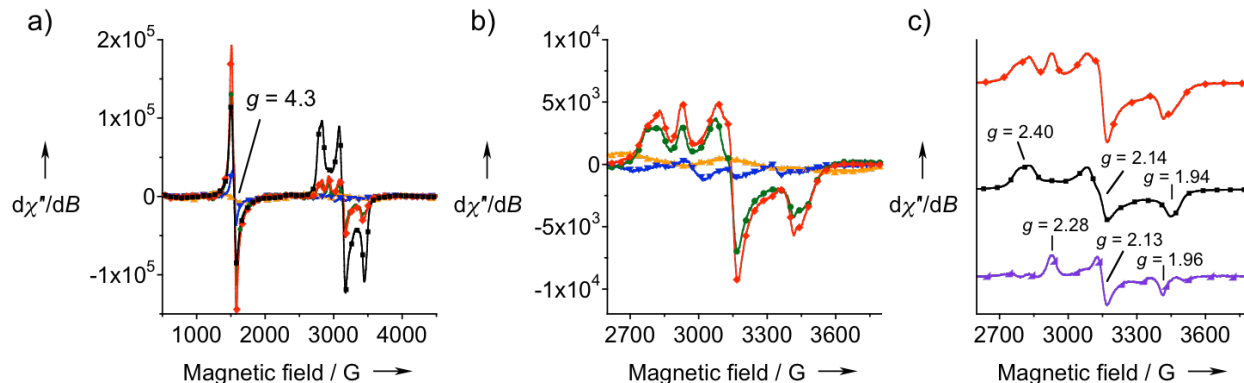


**Figure S5.** EPR spectra of the reaction of 1.0 mM **1** in CH<sub>3</sub>CN at -20 °C with 0.5 equiv of H<sub>2</sub>O<sub>2</sub>. a) EPR spectra (recorded at 4 K) of frozen samples of 1.0 mM solutions of **1** (blue inverted triangles) and **2** (orange triangles) in CH<sub>3</sub>CN and of samples of the reaction of 1.0 mM **1** with 0.5 equiv of H<sub>2</sub>O<sub>2</sub> (in CH<sub>3</sub>CN at -20 °C) frozen at *ca.* 22 min (green circles) and at nearly complete decay of **1** (*ca.* 100 min, red diamonds). Also shown is the EPR spectrum of independently generated **3** (1.0 mM in acetone, black squares). EPR signals shown in a) were magnified by a factor of five except for that of **3**. b) Expanded view of the region from 2600 to 3800 G. c) Difference EPR spectrum (purple right-angled triangles) generated by subtraction of the spectrum of **3** (reduced by a factor of 25, black squares) from that of the reaction mixture (*ca.* 100 min, red diamonds).

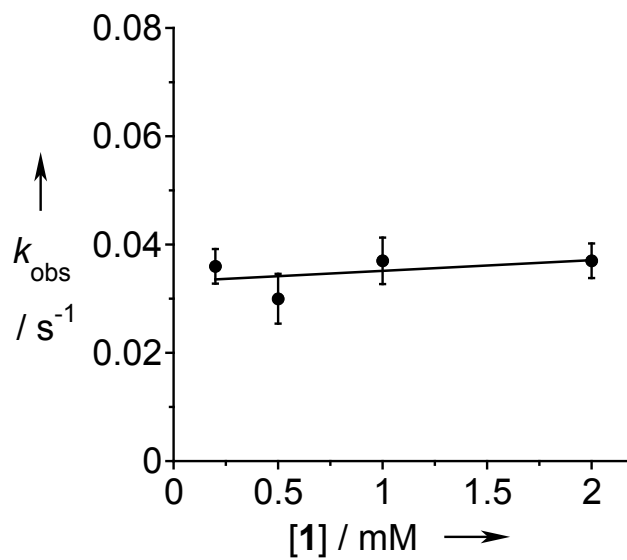


**Figure S6.** Plot of the pseudo-first-order rate constant ( $k_{\text{obs}}$ ) versus [1] (0.2 – 2.0 mM) for the reaction of **1** with 50 mM H<sub>2</sub>O<sub>2</sub> in CH<sub>3</sub>CN at –20 °C.

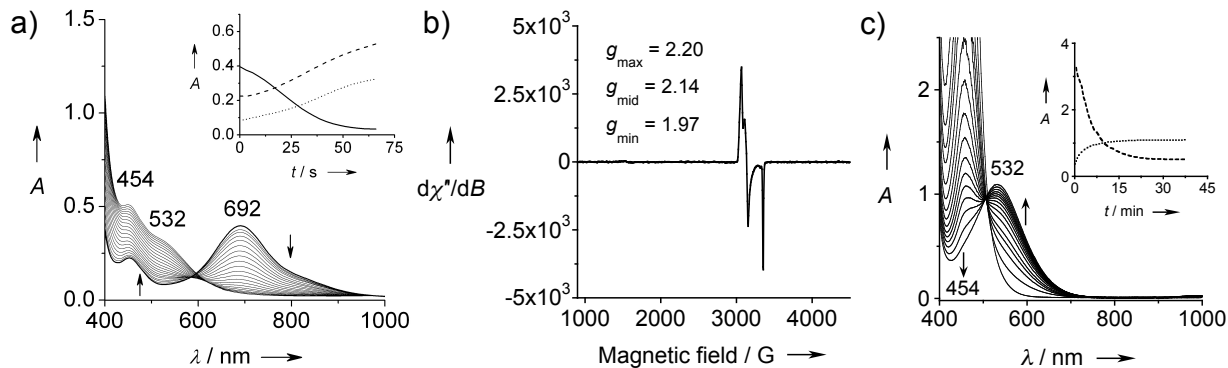


**Figure S7.** Evidence for the formation of **6** in the reaction of **1** with an excess of  $\text{H}_2\text{O}_2$ . a) UV-Vis spectra of the first 1 min of the reaction of 1.0 mM **1** in  $\text{CH}_3\text{CN}$  (bold line) with 50 equiv of  $\text{H}_2\text{O}_2$  at  $-20\text{ }^\circ\text{C}$  (path length, 1.0 cm). Inset: Time courses of the decay of **1** ( $\lambda = 692\text{ nm}$ , solid line), formation of **2** ( $\lambda = 454\text{ nm}$ , dashed line), and formation of **6** ( $\lambda = 532\text{ nm}$ , dotted line). b) EPR spectrum of a sample obtained upon consumption of **1** in the reaction of 1.0 mM **1** with 20 equiv of  $\text{H}_2\text{O}_2$  (in  $\text{CH}_3\text{CN}$  at  $-20\text{ }^\circ\text{C}$ ). This spectrum was recorded at 77 K under non-saturating conditions with the instrument operating at 9.26 GHz, a power of 20.5 mW, a modulation frequency of 100 kHz, a modulation amplitude of 10 G, and a resolution in the X direction of 1024 points. c) UV-Vis spectra of the formation of **6** ( $\lambda_{\text{max}} = 532\text{ nm}$ ) upon the addition of 700 equiv of  $\text{H}_2\text{O}_2$  to 1.0 mM **2** in  $\text{CH}_3\text{CN}$  at  $-20\text{ }^\circ\text{C}$  (path length, 1.0 cm). Inset: Time courses of the decay of **2** ( $\lambda = 454\text{ nm}$ , dashed line) and formation of **6** ( $\lambda = 532\text{ nm}$ , dotted line).

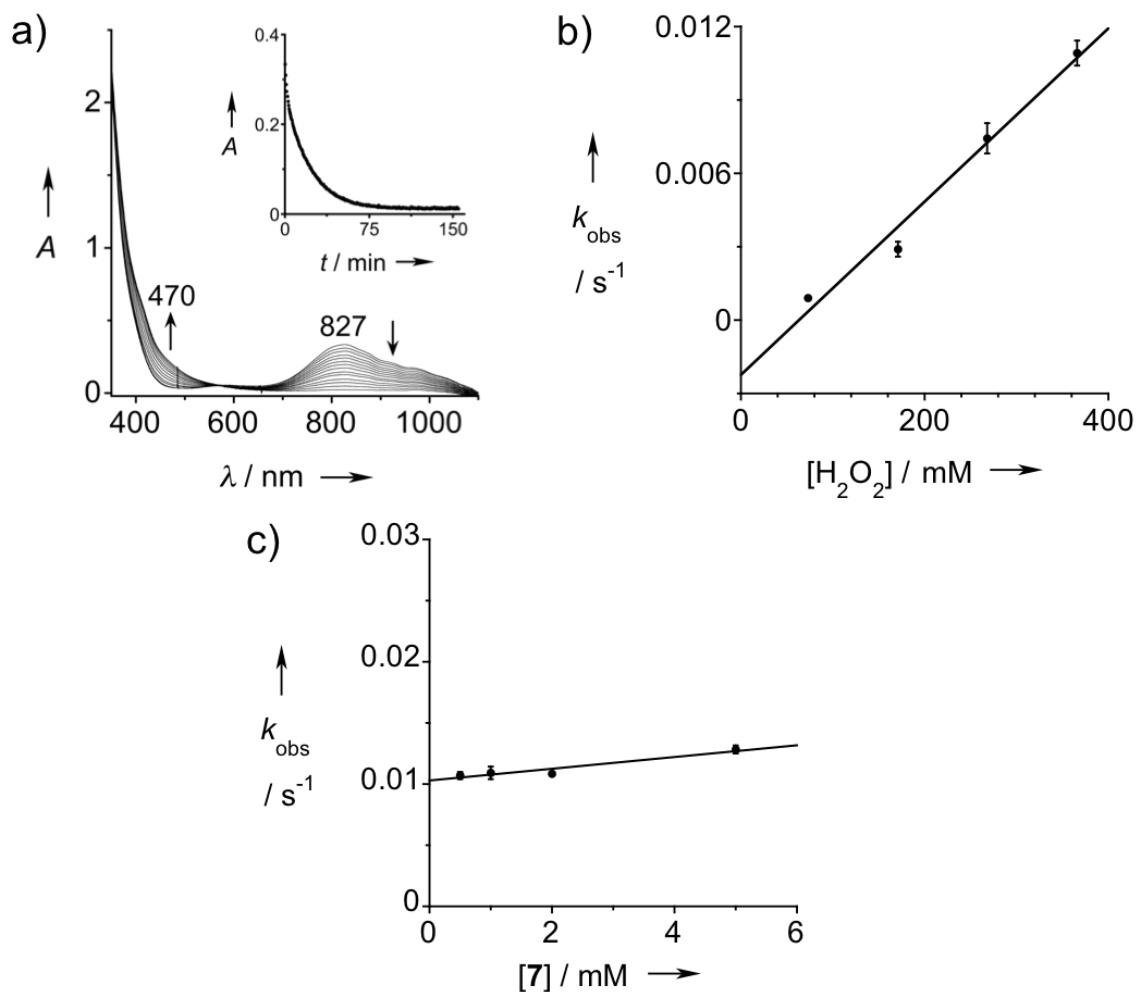


**Figure S8.** Kinetic results for the reaction of 7 with H<sub>2</sub>O<sub>2</sub> in CH<sub>3</sub>CN at 25 °C. a) UV-Vis spectra of the reaction of 1.0 mM 7 in CH<sub>3</sub>CN (λ<sub>max</sub> = 827 nm) with 75 equiv of H<sub>2</sub>O<sub>2</sub> (path length, 1.0 cm). Inset: Time course of the reaction (λ = 827 nm). b) Plot of  $k_{\text{obs}}$  versus [H<sub>2</sub>O<sub>2</sub>] (73 – 366 mM) for the reaction of 1.0 mM 7 with H<sub>2</sub>O<sub>2</sub>. c) Plot of  $k_{\text{obs}}$  versus [7] (0.5 – 5.0 mM) for the reaction of 7 with 366 mM H<sub>2</sub>O<sub>2</sub>.